End-pumped Nd:YVO_4 laser with reduced thermal lensing via the use of a ring-shaped pump beam

DI LIN*, **W ANDREW CLARKSON**

Optoelectronics Research Centre, University of Southampton, Southampton, SO17 1BJ, UK
**Corresponding author: Di.Lin@soton.ac.uk*

Received XX Month XXXX; revised XX Month, XXXX; accepted XX Month XXXX; posted XX Month XXXX (Doc. ID XXXXX); published XX Month XXXX

A simple approach for alleviating thermal lensing in end-pumped solid-state lasers using a pump beam with a ring-shaped intensity distribution to decrease the radial temperature gradient is described. This scheme has been implemented in a diode-end-pumped Nd:YVO_4 laser yielding 14 W of TEM_{00} output at 1.064 µm with a corresponding slope efficiency of 53% and a beam propagation factor (M^2) of 1.08 limited by available pump power. By comparison, the same laser design with a conventional quasi-top-hat pump beam profile of approximately equal radial extent yielded only 9 W of output before the power rolled over due to thermal lensing. Further investigation with the aid of a probe beam revealed that the thermal lens power was ~30% smaller for the ring-shaped pump beam compared to the quasi-top-hat beam. The implications for further power scaling in end-pumped laser configurations are considered.

OCIS codes: *(140.3580) Lasers, solid-state; (140.3410) Laser resonators; (140.6810) Thermal effects.*

http://dx.doi.org/10.1364/OL.99.099999

Diode-pumped solid-state lasers with end-pumped rod geometries have become very popular for a wide range of applications owing to their high efficiency, compactness, flexibility in mode of operation, and excellent fundamental transverse mode (TEM_{00}) beam quality. However, the requirement for a small pump beam size makes scaling end-pumped lasers to higher powers rather challenging due to the high heat loading density within the laser medium, which leads to a strong spatial variation in temperature over the pumped region. This, in turn, leads to strong thermal effects, notably highly aberrated thermal lensing, which degrades beam quality and reduces efficiency, ultimately limiting power scalability. A number of techniques have been developed to reduce adverse thermal lensing effects in end-pumped rod lasers, including the use of lower quantum defect pumping schemes [1], composite (end-capped) laser crystals [2], double-end pumping configurations [3] and multiple gain crystals [4].

Here, we present an alternative strategy for reducing thermal lensing, which could in principle be used in conjunction with these schemes to facilitate further power scaling. Our approach utilizes a pump beam with a ring-shaped intensity profile to yield a central (unpumped) region in the laser mode where there is no heat dissipated. The net result is a more uniform temperature distribution 'averaged' over the laser mode and hence considerably weaker thermal lensing compared to a more traditional quasi-top-hat pump beam profile (e.g. from a fiber-coupled diode pump laser). Moreover, beam distortion is only experienced in the wings of the laser mode leading to weak aberration-induced degradation in beam quality. Inevitably, there is a compromise between weaker thermal lensing and higher threshold pump power due wing-pumping favoring the use of high-gain four-level laser transitions.

The temperature distribution in a solid-state laser rod, and hence the resulting thermal effects, strongly depend on the pump deposition profile. This is illustrated in Fig. 1(b), which shows calculated normalized temperature profiles in an end-pumped, edge-cooled laser rod for two different pump beam profiles under the assumption of purely radial heat flow. The black curve in Fig. 1(a) shows the normalized one dimensional intensity profile for a 'top-hat' pump beam profile with intensity $I_p(r,z)$ is given by:

$$I_p(r,z)=\begin{cases} P_p(z)/\pi r_b^2 , & r\le r_b \\ 0 , & r>r_b \end{cases} \tag{1}$$

where $P_p(z)$ is the pump power at axial position z, r is the radial position, and r_b is the pump beam spot size radius Whereas, the red curve shows the normalized one dimensional intensity profile for an idealized ring-shaped pump beam which has an outer radius r_b and an inner radius r_a with a step-like intensity profile given by:

$$I_p(r,z)=\begin{cases} 0 , & r<r_a \\ P_p(z)/\pi\left(r_b^2-r_a^2\right) , & r_a\le r\le r_b \\ 0 , & r>r_b \end{cases} \tag{2}$$

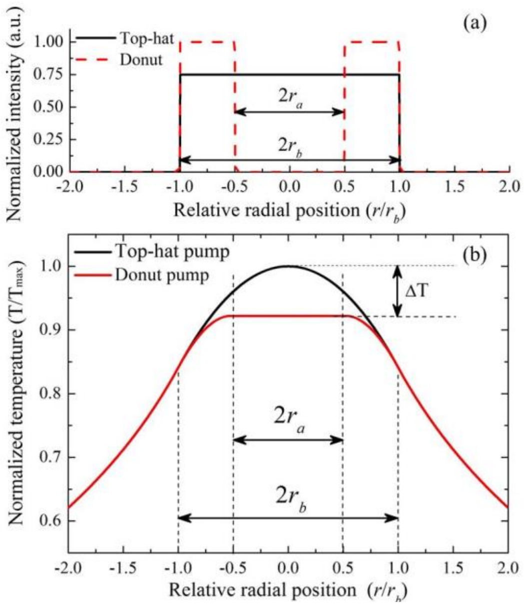

Fig. 1. (Color online) (a) Normalized radial intensity distributions for an ideal top-hat pump and donut-shaped pump profiles with r_b/r_a=2; (b) the corresponding normalized temperature profiles for an end-pumped edge-cooled gain medium.

In both cases the temperature profile is normalized with respect to the maximum temperature reached at the center of the laser rod for a top-hat pump profile. It is immediately apparent that the maximum temperature rise for the donut pump beam is somewhat smaller than for the top-hat pump beam. For purely radial heat flow, it can be shown that this difference in temperature ΔT is given by:

$$\Delta T = \frac{P_p(z)\alpha_p\gamma_h}{4\pi K_c}\left[\frac{2}{\chi^2-1}\log_e \chi\right] \quad (3)$$

where α_p is the absorption coefficient for pump light, γ_h is the fraction of absorbed pump converted to heat, K_c is the thermal conductivity of the gain medium and $\chi=r_b/r_a$ is the aspect ratio. Hence ΔT increases as the aspect ratio of the pump beam is decreased reaching a maximum value of $P_p(z)\alpha_p\gamma_h/4\pi K_c$. This serves as a good illustration of the importance of the pump beam profile in determining the maximum temperature rise. Fig. 2 shows the corresponding normalized thermal lens power as a function of radial position for top-hat and donut pump beam profiles. The thermal lens power is zero over the central (unpumped) portion of the donut pump and hence on average the thermal lens power is much smaller than for the top-hat pump beam averaged over the entire pump profile. It can be seen that the thermal lens strength can be further reduced by decreasing the donut beam's aspect ratio albeit at the expense of reduced gain. Thus, a compromise is needed between the desire for reduced thermal lensing and a low threshold pump power, which favors four-level transitions with high values for emission cross-section and upper-state lifetime.

The use of ring-shaped pumping was investigated for an end-pumped $Nd:YVO_4$ laser (shown in Fig. 3). A simple Z-fold four-mirror resonator was employed comprising a plane pump input mirror (IC) with high reflectivity (>99.8%) at the lasing wavelength (1.064 μm) and high transmission (>95%) at the pump wavelength

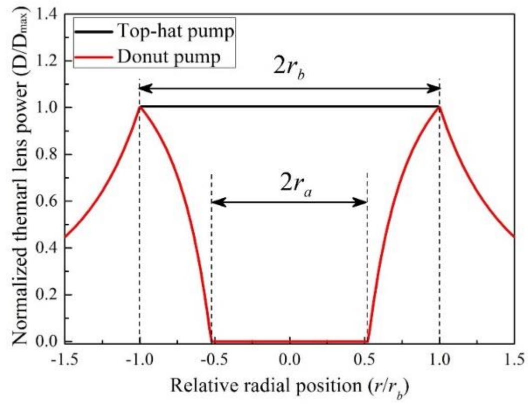

Fig. 2. (Color online) Normalized thermal lens power for an end-pumped edge-cooled gain medium with a top-hat pump profile and a donut shaped pump profile with r_b/r_a=2.

(808 nm), two concave mirrors, R1 and R2 with respective radii of curvature, 2000 mm and 500 mm and high reflectivity (>99.8%) at 1.064 μm, and a plane output coupler (OC) with a transmission of 20% at 1.064 μm. An a-cut 10mm long $Nd:YVO_4$ crystal with a Nd^{3+} doping level of 0.1 at.% was used as the gain medium. The latter was mounted in a water-cooled aluminum heat-sink maintained at 18°C and located in close proximity to the pump incoupling mirror. Pump power was provided by a fiber-coupled laser diode at 808nm with a 200μm diameter (0.22 NA) delivery fiber yielding up to 60W of power in a pump beam with a quasi-top-hat beam profile, which the near field intensity profile is shown in Fig. 4(c). A silica capillary fiber with a 200 μm outer diameter surrounded by a low refractive index polymer coating and with a 105 μm diameter inner air hole was employed as a pump beam re-shaping element. Fig. 4(a) shows an example of side view of the tapered capillary fiber, which one end of the capillary fiber was smoothly tapered down with a tapering length of ~25mm to a solid core with a diameter of ~100μm (~0.4NA). Fig. 4(b) shows a typical end view of the capillary fiber perpendicularly cleaved. This allows efficient in-coupling of quasi top-hat shaped pump light from the pump delivery fiber using a simple telescope (f_1=11mm with 0.25NA and f_2=4mm with 0.62NA) and yielding up to ~ 48 W of pump output from the opposite end

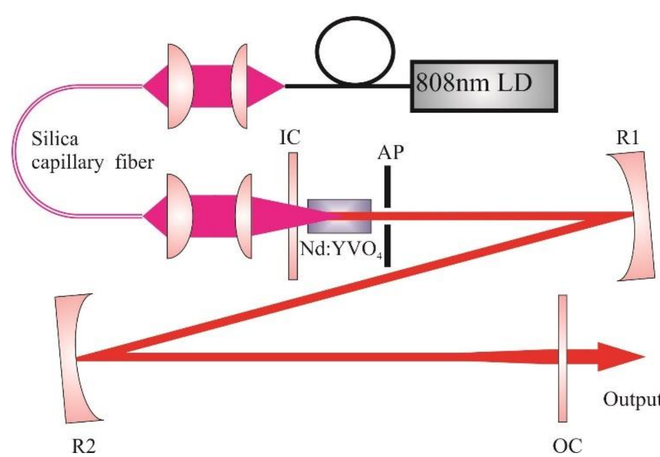

Fig. 3. (Color online) Diode-end-pumped $Nd:YVO_4$ laser configuration with ring-shaped pump beam.

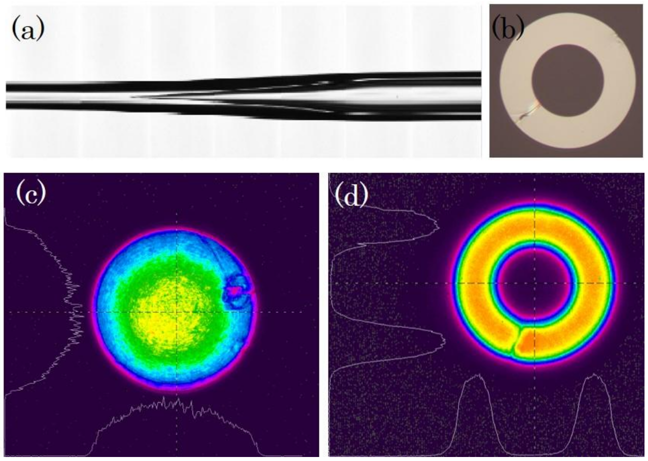

Fig. 4 (a) The side view of tapered, and (b) end-facet of perpendicularly cleaved capillary fiber. The near-field intensity profiles of (c) quasi-top-hat pump beam, and (d) ring-shaped pump beam.

with a ring-shaped near-field beam profile as shown in Fig. 4(d), corresponding to a total coupling efficiency of ~80%. A telescope with a magnification factor of 4 was used to relay image the ring-shaped near field beam profile into the $Nd:YVO_4$ crystal yielding a pump beam with an outer radius (r_b) of ~400 μm and an inner radius (r_a) of ~200 μm. With this arrangement up to 40 W of ring-shaped pump power could be launched into the $Nd:YVO_4$ crystal. The resonator mirrors were positioned to yield negligible astigmatism and a nearly circular fundamental transverse (TEM_{00}) mode with calculated waist radius on the pump incoupling mirror of approximately 380 μm. The resulting total cavity length was ~630 mm. This ensures an adequate spatial overlap of the outer portion of the TEM_{00} mode with the ring-shaped inversion distribution in the gain medium. However, one important consequence of employing such pumping scheme is that the threshold for the higher order LG_{01} donut mode is lower than for the TEM_{00} mode by virtue of it has a better spatial overlap with the inversion distribution. Hence, an aperture (AP) with a hole diameter of 1.1 mm was also inserted into the resonator behind the $Nd:YVO_4$ crystal to suppress the LG_{01} mode whilst maintaining low residual resonator loss for the TEM_{00} mode.

The performance of the $Nd:YVO_4$ laser was investigated for both a ring-shaped pump beam (as shown in Fig. 3) and for a quasi-top-hat pump beam (i.e. without the pump re-shaping capillary fiber). In the latter case the pump beam conditioning lenses were selected to yield a quasi-top-hat beam profile with the same beam radius of 400 μm as used for ring-shaped pumping. Fig. 5 shows the measured laser output power as a function of absorbed pump power for both cases. For the quasi-top-hat pump beam, the $Nd:YVO_4$ laser had a threshold pump power (absorbed) of 2.5 W and above threshold the output power increases linearly with pump power to ~9 W with a corresponding slope efficiency with respect to absorbed pump power of 57.3%. Further increase in pump power beyond ~19 W resulted in a roll-over in output power attributed to thermal lensing and an associated increase in cavity loss due to clipping at the aperture. The maximum output power reached 9.8 W at 23.8 W of absorbed pump power and the M^2 parameter for the output beam at the 9 W power level was measured to be 1.08 confirming near-diffraction-limited TEM_{00} operation.

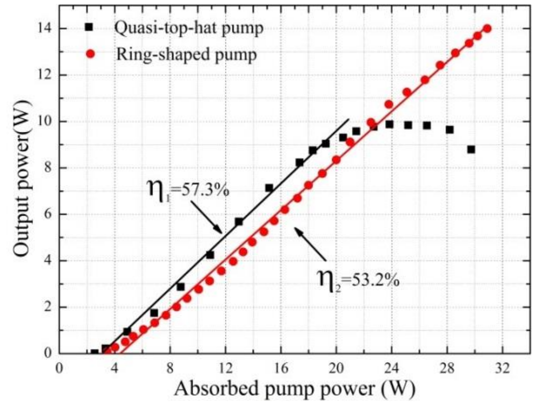

Fig. 5. (Color online) TEM_{00} output power versus absorbed pump power for quasi-top-hat and ring-shaped pump distributions.

By contrast, the threshold pump power (absorbed) for the ring-shaped pump beam was slightly higher at 3.2W due to the poorer pump-laser mode spatial overlap, but the output power increased linearly with pump power to ~14 W limited only by the maximum available pump power (~31 W absorbed). The corresponding slope efficiency was 53.2% with no evidence of a roll-off in power. The M^2 parameter was measured to be 1.06 at maximum power confirming diffraction-limited beam quality. The slightly lower slope efficiency can be attributed to the poorer spatial overlap of the pump beam and laser mode, and the dramatic increase in output power with absence of roll-over is a direct consequence of weaker thermal lensing with the ring-shaped pump beam.

To further confirm the influence of the different pump beam profiles on thermal lensing a simple probe beam experiment was performed using the experimental set-up shown in Fig. 6. In this arrangement the $Nd:YVO_4$ crystal employed in the laser set-up (see Fig. 3) was mounted and supplied with pump power in an identical manner (i.e. with a ring-shaped or quasi-top-hat near-field beam profile), but without the resonator present. The probe beam was provided by a low-power (~100 mW) diode-pumped Nd:YAP laser with a TEM_{00} (M^2=1.01) output at a wavelength of 1.08 μm. This was coupled into the pumped $Nd:YVO_4$ gain medium with the aid of a dichroic mirror with high reflectivity at 1.08 μm and high transmission at the diode pump wavelength (~808 nm) at 45° incidence angle, and aligned to be collinear with the diode pump beam in the $Nd:YVO_4$ crystal. The probe beam waist radius was carefully adjusted using an appropriate arrangement of lenses to be ~380 μm, so that it matched the TEM_{00} beam waist radius used in laser resonator of Fig. 3. The probe beam exiting the $Nd:YVO_4$ crystal (after removal of residual pump light) was analyzed to measure any

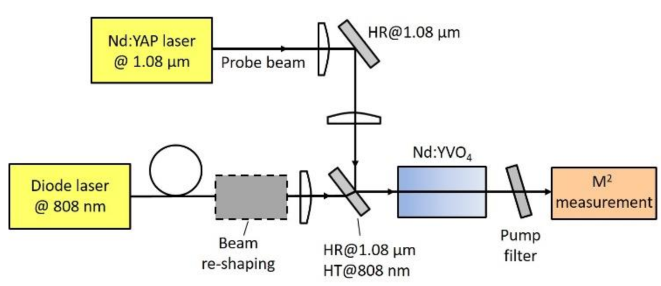

Fig. 6. (Color online) Probe beam set-up for measuring degradation in beam quality and thermal lensing in the end-pumped $Nd:YVO_4$ crystal.

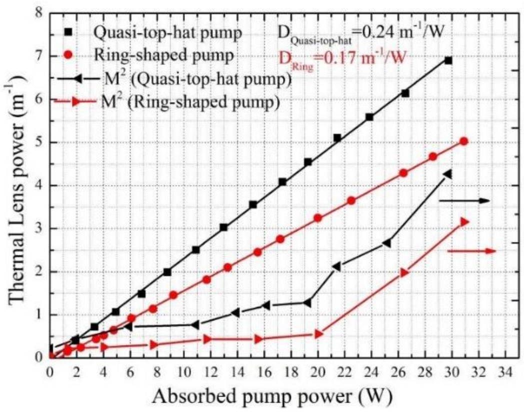

Fig. 7. (Color online) Measured thermal lens power and degradation in probe beam quality versus absorbed pump power with quasi-top-hat and ring-shaped pump beam distributions.

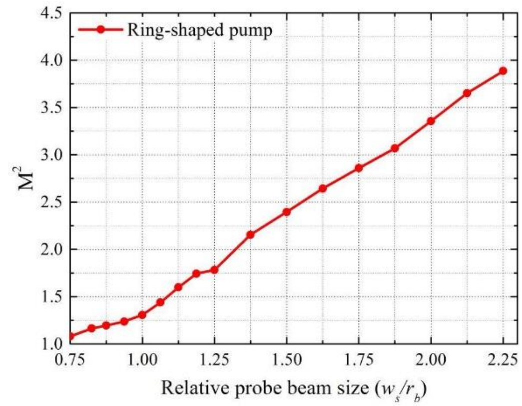

Fig. 8 (Color online) Measured degradation in probe beam quality versus relative probe beam size (w_s/r_b) in the condition of ring-shaped pump beam with ~31 W absorbed pump power.

degradation in the M^2 parameter due to thermally-induced phase aberration and from this the focal length of the thermal lens in the $Nd:YVO_4$ crystal was deduced. Fig. 7 shows the resulting M^2 parameters and thermal lens power as a function of absorbed pump power for ring-shaped and quasi-top-hat pump beams. It can be seen that at the highest pump power (~31 W absorbed) the M^2 parameter for the probe beam degrades to ~1.23 for the ring-shaped pump beam compared to ~1.32 for the quasi-top-hat beam, suggesting that the impact of thermally-induced phase aberration on beam quality is comparable for the two pump distributions. The more severe degradation in beam quality for the quasi-top-hat pump beam than the indication for the idealized top-hat pump beam in the Fig. 2 can be attributed to the non-uniform intensity distribution of the former as shown in Fig. 4(c) and hence the presence of non-parabolic phase distortion. The thermal lens power increases with pump power at ~0.24 m^{-1}/W for the quasi-top-hat pump and 0.17 m^{-1}/W for the ring-shaped pump. Hence the thermal lens power is ~30% stronger for the quasi-top-hat pump beam. This confirms that the output power roll-over for the $Nd:YVO_4$ laser pumped by a quasi-top-hat pump beam is a consequence of stronger thermal lens which acts to increase the laser mode size in the vicinity of the aperture increasing resonator loss due to clipping as the laser operation is shifted towards the unstable region.

The impact of the relative probe beam size (w_s/r_b) on the M^2 parameters was analyzed under the condition of the ring-shaped pump at the maximum absorbed pump power. In this case, the probe beam waist radius in the $Nd:YVO_4$ crystal adjusted from 300μm to 900μm, corresponding to a relative beam size of 0.75 to 2.25, and the resultant M^2 parameters are shown in Fig. 8. It is apparent that the probe beam only experiences slight degradation in the beam quality that the M^2 parameters vary from 1.08 to 1.30 when $w_s/r_b < 1$, whereas, the probe beam dramatically degrades in the beam quality with the further increase of the beam size. This indicates that the thermally-induced phase aberration is only relatively weak within the pump beam region and requires the laser beam size to be smaller than the pump beam size to avoid any severe beam distortion for the laser beam.

In conclusion, we have demonstrated the use of a ring-shaped pump beam in combination with an aperture to selectively generate the TEM_{00} mode in an end-pumped $Nd:YVO_4$ laser with high efficiency. This unique pump beam geometry yields a significant reduction in thermal lens strength compared to the more traditional quasi-top-hat pump beam profile used in end-pumped lasers. Further optimization of the ring-shaped pump beam profile to yield even weaker thermal lensing at the expense of a higher threshold pump power should allow scaling to even high powers whilst maintaining diffraction-limited TEM_{00} beam quality and high efficiency. This novel approach for mitigation of thermal lensing is well suited to four-level lasers (e.g. $Nd:YVO_4$) with a high value for the product of emission cross-section and upper-state lifetime.

The data from this paper can be obtained from University of Southampton e-Prints repository Dataset 1, Ref. [5].

Funding:

European Commission under the Seventh Framework Programme (HALO project no. 314410).

References

1. L. McDonagh, R. Wallenstein, R. Knappe, and A. Nebel, Opt. Lett. **31**, 3297 (2006).
2. Z. Xiong, Z. G. Li, N. Moore, W. L. Huang, and G. C. Lim, IEEE J Quantum Electron. **39**, 979 (2003).
3. H. Ogilvy, M. J. Withford, P. Dekker, and J. A. Piper, Opt. Express **11**, 2411 (2003).
4. Y. F. Chen, Y. P. Lan, and S. C. Wang, Opt. Letters **25**, 1016 (2000).
5. https://doi.org/10.5258/D0108.

References

1. L. McDonagh, R. Wallenstein, R. Knappe, and A. Nebel, "High-efficiency 60 W TEM00 Nd : YVO4 oscillator pumped at 888 nm," Optics Letters **31**, 3297-3299 (2006).
2. Z. Xiong, Z. G. Li, N. Moore, W. L. Huang, and G. C. Lim, "Detailed investigation of thermal effects in longitudinally diode-pumped Nd : YVO4 lasers," IEEE J Quantum Elect **39**, 979-986 (2003).
3. H. Ogilvy, M. J. Withford, P. Dekker, and J. A. Piper, "Efficient diode double-end-pumped Nd : YVO4 laser operating at 1342nm," Optics Express **11**, 2411-2415 (2003).
4. Y. F. Chen, Y. P. Lan, and S. C. Wang, "Efficient high-power diode-end-pumped TEM00 Nd:YVO4 laser with a planar cavity," Optics Letters **25**, 1016-1018 (2000).
5. http://dx.doi.org/10.5258/SOTON/XXXX.